Bioorganic & Medicinal Chemistry Letters 20 (2010) 4561–4565

Contents lists available at ScienceDirect

Bioorganic & Medicinal Chemistry Letters

journal homepage: www.elsevier.com/locate/bmcl

# Identification of novel α7 nAChR positive allosteric modulators with the use of pharmacophore in silico screening methods

Anna Maria Capelli [a,*], Laura Castelletti [a], Cristian Salvagno [a], Beatrice Oliosi [a], Elisa Di Lenarda [a,c], Caterina Virginio [a], Andrew Lightfoot [b], James N. C. Kew [b], Simon Teague [b]

[a] GlaxoSmithKline, Molecular Discovery Research, v. Fleming 4 37135 Verona, Italy
[b] GlaxoSmithKline, Neurosciences Centre of Excellence of Drug Discovery, Harlow NFSP, Essex, UK
[c] Novartis Institutes for BioMedical Research (NIBR, Novartis Pharma Schweizerhalle A, Auhafenstrasse, CH-4133 Schweizerhall, Switzerland

ARTICLE INFO

*Article history:*
Received 1 June 2010
Accepted 2 June 2010
Available online 8 June 2010

*Keywords:*
Alpha7 nicotinic
Positive modulator
Pharmacophore

ABSTRACT

The pharmacophore model of in house potent and selective α7 nAChR positive allosteric modulators is reported. The model was used to fish out commercially-available compounds from corporate 3D databases. As a result, novel α7 positive modulator chemotypes were identified. A rat full PK profile of a representative compound is also described.



Nicotinic acetylcholine receptors (nAChRs) belong to the Cys-loop receptor superfamily of cationic ligand-gated ion channels. Functional receptors are made of five subunits assembled from 17 known homologous polypeptide family members (α1–10, β1–4, γ, δ, and ε). Neuronal nAChRs are expressed throughout the peripheral and the central nervous system as well as in non-neuronal tissues. The α7 nAChRs are homopentamers containing the α7 subunit, characterized by rapid activation and desensitization following exposure to agonists, high $Ca^{2+}$ permeability,[1,2] selective activation by choline[3] and blockade by α-bungarotoxin and methyllycaconitine. Neuronal nicotinic receptors play important roles in modulating neurotransmission, cognition, sensory gating and anxiety.[4] In particular, the α7 nAChR receptor is a therapeutic target for schizophrenia as suggested by linkage studies demonstrating an association between the α7 locus and a sensory gating deficit, a major schizophrenia endophenotype.[5] Considering that receptor activation by agonists including acetylcholine and nicotine is followed by rapid desensitization of the receptor, chronic treatment with agonists may result in tolerance/functional blockade of the receptor.[6] An alternative approach is represented by the use of positive allosteric modulators (PAM) to enhance receptor function elicited by the endogenous ligand without directly activating or desensitizing the receptor. Several positive modulator chemotypes had been reported in the literature,[7] three of these have also been characterized in vivo: PNU-120596[8] from Pfizer, 'compound **6**'[9] from the University of California and NS1738[10] from Neurosearch (Fig. 1). These compounds demonstrated activity in a number of animal models and, hence, they are of potential value to treat a variety of disorders like Alzheimer's disease, inflammation and schizophrenia.

We approached the identification of novel PAMs initially through the screening of in house compound collections with the use of a FLIPR (Fluorescent Imaging Plate Reader) $Ca^{2+}$ assay based on a GH4C1 cell line stably expressing the human α7 nAChR produced as described in.[11,12]

As a result, novel chemotypes belonging to the chemical class of phthalazinones, pyridazinones and quinazolines (lead series) were

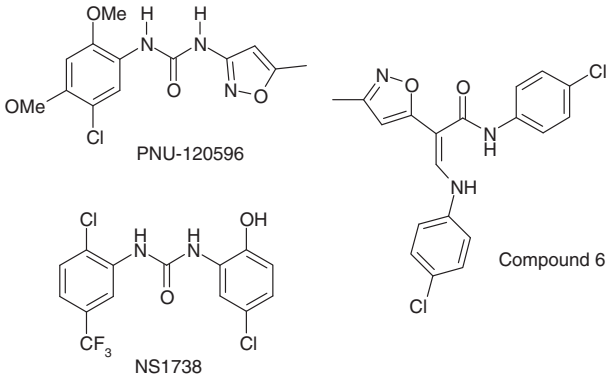


**Figure 1.** α7 positive modulators characterized in vivo animal models.

* Corresponding author.
*E-mail address:* Anna-Maria.M.Capelli@gsk.com (A.M. Capelli).

0960-894X/$ - see front matter © 2010 Elsevier Ltd. All rights reserved.
doi:10.1016/j.bmcl.2010.06.014

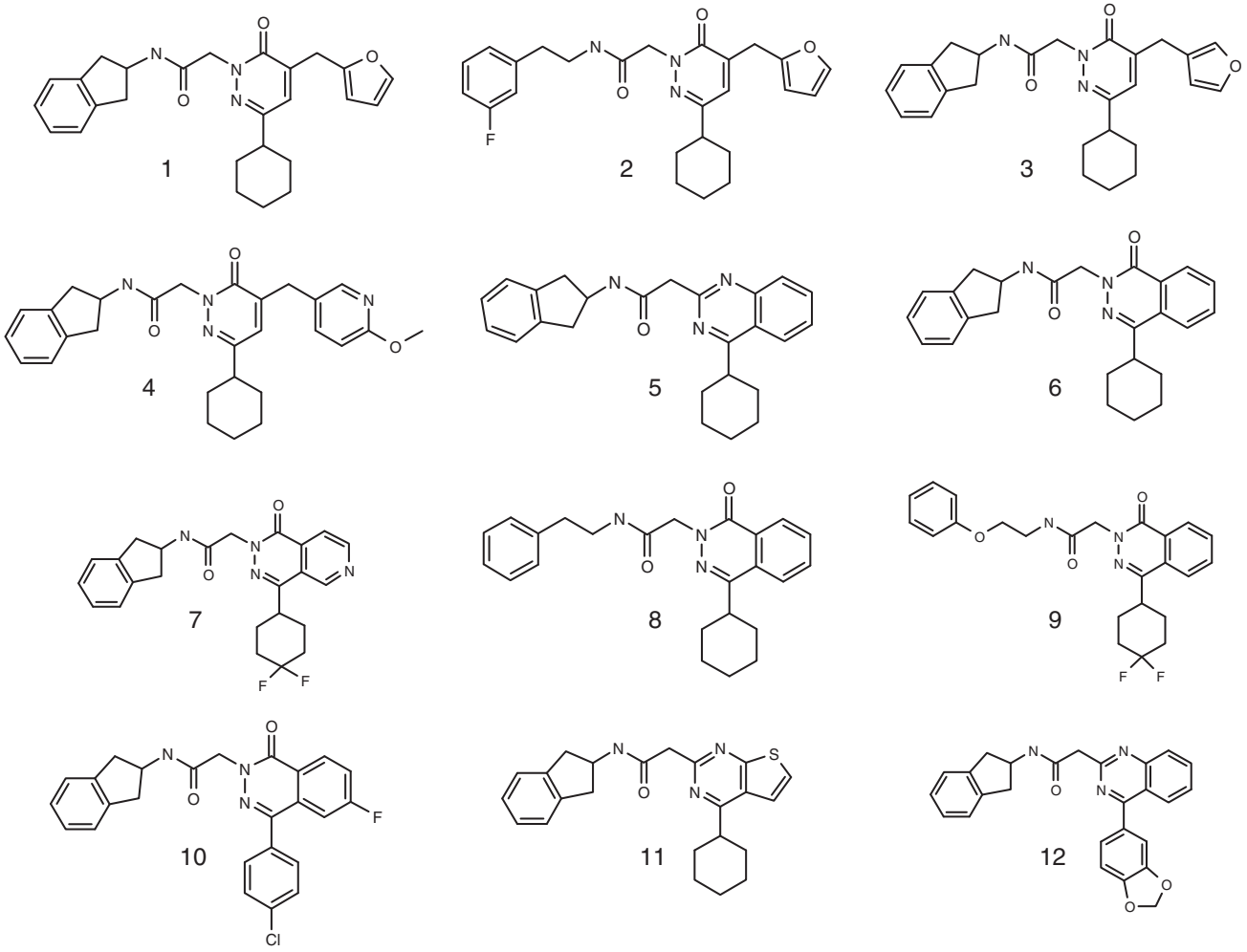


**Figure 2.** Representative in house α7 positive modulators identified by FLIPR focused screening activities.

identified. Representative compounds from these series are shown in Figure 2. These derivatives exhibited good potency and potentiation in the in vitro FLIPR assay (Table 1).

**Table 1**
In vitro potency and potentiation of representatives α7 positive modulators reported in Figure 2 and PNU-120596

| Compds | Potency $pEC_{50}$[a] | Potentiation Asym_max[b] (%) | ACD-log $P$[c] |
|---|---|---|---|
| PNU-120596 | 6.8 (±0.2) | 114 (±23) | 1.5 |
| **1** | 8.7 (±0.1) | 129 (±20) | 1.7 |
| **2** | 8.7 (±0.1) | 107 (±13) | 1.5 |
| **3** | 8.5 (±0.3) | 136 (±29) | 2.4 |
| **4** | 8.0 (±0.2) | 136 (±27) | 2.4 |
| **5** | 8.2 (±0.3) | 102 (±3) | 4.7 |
| **6** | 8.1 (±0.4) | 135 (±28) | 3.1 |
| **7** | 8.0 (±0.1) | 132 (±16) | 2.1 |
| **8** | 8.0 (±0.3) | 150 (±39) | 2.9 |
| **9** | 7.5* (±0.2) | 96 (±6) | 2.5 |
| **10** | 7.6* (±0.3) | 108 (±12) | 4.0 |
| **11** | 7.6* (±0.2) | 126 (±37) | 4.7 |
| **12** | 7.6 (±0.4) | 93 (±9) | 4.5 |

[a] Values are means of at least three experiments, except for * where $n = 2$; standard deviation is given in parentheses. Results were achieved in agreement to the procedure described in Ref. 11.
[b] Asym_max is expressed as percentage (%) of the fitted potentiation compared to an unpublished GSK internal positive modulator standard.
[c] Calculated log $P$ with ACD v.11.

A further characterization of these compounds was performed using whole-cell voltage-clamp electrophysiology on the same cell line. Receptor activity was evoked in response to 100 μM acetylcholine in the absence and presence of increasing concentrations of test compound.[12] Electrophysiological examination of compound **1** showed a $pEC_{50}$ of 8.4, a value in good agreement with FLIPR data ( Fig. 3). In addition, these derivatives demonstrated selectivity over other nicotinic subtypes, like α1 involved in the electromechanical coupling of nerve and muscle, and the 5-$HT_3$ receptor, a member of the superfamily of cys-loop ligand-gated ion channels like nicotinic receptors, for which antagonist treatment could be associated with serious gastrointestinal adverse effects. This is exemplified by compound **1** which showed $pIC_{50}$ = 6.1 ± 0.3 ($n = 10$), $pIC_{50} = 6 \pm 0.2$ ($n = 3$), and $pIC_{50} = 5.1 \pm 0.08$ ($n = 2$) when tested in antagonist mode using a FLIPR assay with human α1 TE671, human α3 IMR32 and human 5-$HT_3$ receptor cell line, respectively.

As shown in Table 1, some derivatives are characterized by high calculated lipophilicity and poor solubility as exemplified by compound **5** (equilibrium water solubility <1 μg/mL) and compound **11** (equilibrium water solubility = 0 μg/mL); moreover these structures showed high MW and flexible side-chains resulting in poor starting points for a medicinal chemistry exploration.

Despite the SAR information generated on these derivatives (e.g., the crucial role of the carbonyl group/quinazoline nitrogen –N1– in the core, the importance of the lipophilic pendant groups and the need for an acidic hydrogen in the chain), it was not

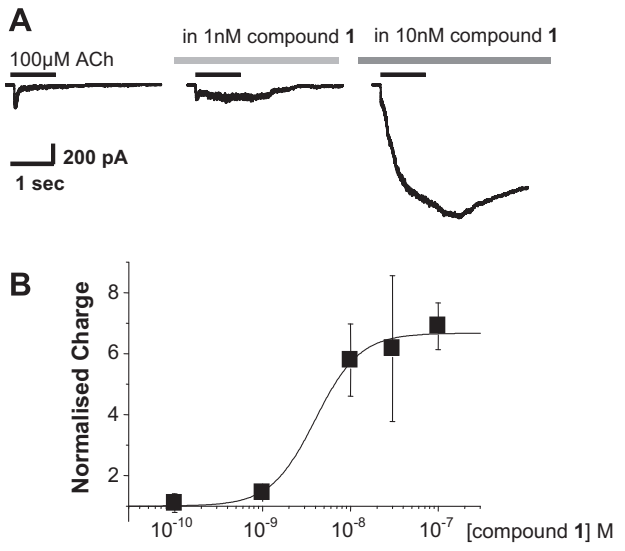


**Figure 3.** Whole-cell voltage-clamp recordings and concentration–response curve from α7-GH4C1 cells. (A) ACh-induced currents recorded from a cell in the absence (left panel) and presence of the indicated concentrations (middle and right panels) of compound **1**. (B) Electrophysiological concentration–response curve (CRC) for derivative **1**. The vertical axis reports the 'Normalized Charge' parameter, the charge measured during 100 μM ACh application in the presence of increasing concentrations of compound **1**, normalized to the response elicited in the same cell by the application of ACh alone. Data points were fitted to the Hill equation. Each data point represents the means ± sem of up to six cells. The $pEC_{50}$ value was 8.4 and the maximum activated current as % of ACh-evoked current was 690% at 100 nM.

possible to achieve the desired parameters for a full progression of this series.

Accordingly, despite the existence of these potent in vitro structures, it was crucial to identify new and more tractable chemotypes.

Pharmacophore modeling was extensively applied as part of an integrated medicinal and computational chemistry strategy aimed at this objective. A small set of the newly identified structures and characterized by high potency in the α7 positive modulator FLIPR assay ($pEC_{50}$ >7.5) was selected to build the model assuming that they bind to the α7 receptor with a common binding mode according to the available SAR. Representative examples of the compounds included in the study are shown in Table 1.

All pharmacophore modeling work was performed with program Catalyst.[13] Ligand conformational searches were carried out using the FAST routine (max 255 conformations), while common-feature alignments were performed using the HipHop algorithm implemented in Catalyst.[13] Standard Catalyst pharmacophore features (H-bond acceptor, H-bond donor, aromatic rings, hydrophobic groups) were selected according to the SAR data available in house for these compound series. Among the different top scoring pharmacophore solutions generated by the program, the most satisfactory models were chosen according to the quality of ligand conformations, the RMS deviation of the ligand conformations to pharmacophore features and common volumes. In Figure 4 the best pharmacophore model obtained is shown superimposed with some representative compounds included in the study. The model consists of an HB-donor mapped by the side chain amide NH moiety (purple spheres), an HB-acceptor (green spheres) mapped by the carbonyl group in the core and of three hydrophobic regions (cyan spheres).

The model is qualitatively consistent with the SAR data available for this compound series and its ability to identify novel chemotypes was assessed by running in silico screening exercises on a random set of corporate database compounds seeded with some phthalazinone/pyridazinones/quinazolines derivatives not included in the model generation.[14]

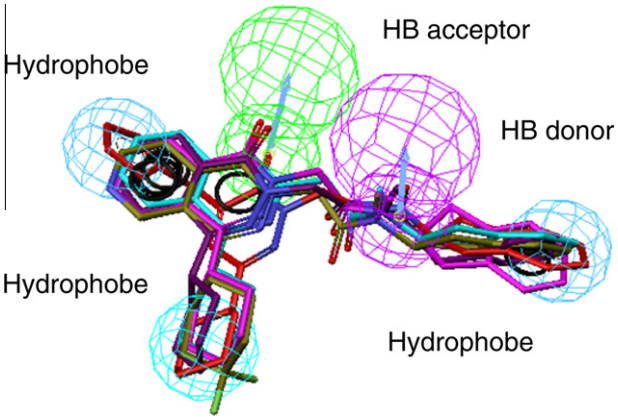


**Figure 4.** Pharmacophore model generated with the compounds **1**–**12**. All the structures are shown fitted to the model. Color coding of the pharmacophoric features: green, H-bond acceptor; purple, HB-donor; cyan, hydrophobic region.

Subsequently, the best pharmacophore solution was used to carry out in silico screening exercises following two approaches.

In the first approach, the model was used to search a 3D database of commercially-available compounds using Catalyst. About 6000 structures mapping the pharmacophore were retrieved. Subsequently, they were prioritized according to their fit to the pharmacophore model, calculated with the Citest routine distributed with Catalyst. The shape similarity of their best mapping conformations was then calculated with the use of ROCS[15] with respect to that of the best mapping conformations of the compounds used to generate the pharmacophore model (Fig. 3). The Tanimoto (shape) similarity threshold was set to 0.7. The ranked list of compounds was subsequently pruned with the use of a statistical model of CNS brain penetration developed in house, leading to a final list of 104 compounds purchased.

In the second approach, the shape of the best mapping conformations of five representative scaffolds used to generate the model was exploited to carry out a pure shape-based search within a 3D database of commercially-available compounds with the use of ROCS. The 1000 top scoring derivative hitlist was then pruned using the same CNS brain penetration model mentioned above. Finally, the hitlist compounds belonging to the lead series chemical class were removed with the use of structural filters[16] leading to a final set of 91 compounds purchased and then tested in the α7 FLIPR assay.

In a third in silico screening exercise, 424 representative α7 positive modulators, including 32% lead series analogues, were parameterized with the use of 3D Mill pharmacophoric hashed fingerprints[17] and a 3D similarity search was run in the database of commercially-available compounds described in the same way. The hitlist compounds were ranked according to their similarity assessed by Tanimoto * Hamming index.[18] As a result, 110 derivatives, passing also the CNS brain penetration filter, were purchased.

The derivatives selected with the three methods described were then tested in the FLIPR assay in concentration response curve (CRC) mode as summarized in Table 2.

As shown, the use of the pure pharmacophore shape-based search was very effective in fishing out novel α7 positive modulators as judged by the high hit rate and the number of distinct chemotypes found which were structurally unrelated to the derivatives used to build the model. In addition, there is no overlap among the three different hitlists. In light of these results, it seems reasonable to conclude that compounds need to map only a subset of the five pharmacophoric features to achieve $pEC_{50}$ values between 5 and 6.

**Table 2**
Performance of the pharmacophore approaches used to carry out the in silico screening exercises of commercially-available compounds

| Search method | # of actives[a] | Hit rate (%) | No. of chemotypes[b] |
|---|---|---|---|
| 1. 3D pharmacophore query + shape | 7 | 6.7 | 5 |
| 2. Shape-based pharmacophore | 13 | 14 | 12 |
| 3. 3D pharmacophore similarity | 3 | 3 | 3 |

[a] Number of α7 positive modulators characterized by FLIPR $pEC_{50}$ >5.
[b] Number of Ward clusters.[19]

Among the derivatives fished out by the pure shape-based pharmacophore search, a promising chemical series exemplified by compounds **13** and **14** (Table 3) was selected for further characterization.

These derivatives are structurally unrelated to the compounds used to build the model, which demonstrates the value of this lead hopping exercise. Subsequently, further commercial analogues of this novel chemotype were fished out from in house collection using a 2D similarity search (1024 Daylight 2D hashed fingerprints, Tanimoto index $\geqslant 0.85$). This exercise resulted in particular in the identification of the close analogue **15**, more potent than the reference compounds (**13** and **14**, Table 3) upon the introduction of the methyl group at ortho position of the side chain phenyl ring. The alignment of the newly identified derivate **15** to the pharmacophore model in comparison to derivative **11** is reported in Figure 5. Compound **15** completely misses one of the pharmacophoric points, suggesting the potential to further increase the in vitro potency of these derivatives with an appropriate decoration of the scaffold.

The selectivity profile of derivative **15** versus α1 nAChR ($pIC_{50} = 6.0 \pm 0.3$, $n = 5$), α3 nAChR ($pIC_{50} = 5.6 \pm 0.6$, $n = 4$), α4 nAChR ($pIC_{50} = 6.0 \pm 0$, $n = 3$), and 5-$HT_3$ receptor ($pIC_{50} = 6.0 \pm 0.5$, $n = 4$) was acceptable for a screening hit. Furthermore, considering the low affinity values of these off-target receptors, it might be possible to further optimize the selectivity window of this series during lead optimization activities. In addition, **15** was characterized by a promising in vitro PK profile exemplified by intrinsic clearance (Cli) in human and rat microsomes of 0.6 and 4.1 mL/mg/g, respectively; P450 $IC_{50}$ were greater than 5 μM in CYP1A2-ER, CYP2C9-FCA, CYP2C19-BMC, CYP3A4-7BQ P450_isoforms (Cypex). In light of these data, this compound was progressed to in vivo PK studies.[20]

**Table 3**
In vitro potency and potentiation of the α7 positive modulators fished out from commercial sources with the pharmacophore model

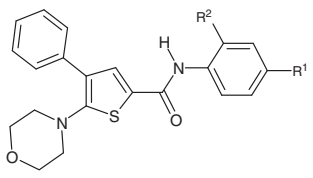


| Compds | R1,R2 | Potency $pEC_{50}$[a] | Potentiation Asym_max[b] (%) |
|---|---|---|---|
| **13** | Me, H | 5.9 (±0.4) | 62 (±26) |
| **14** | F, H | 5.9* (±0.5) | 40 (±1) |
| **15** | Me, Me | 6.8 (±0.3) | 96 (±15) |

[a] Values are means of at least three experiments, except for * where $n = 2$; standard deviation is given in parentheses.
[b] Asym_max is expressed as % fitted potentiation compared to the same internal positive modulator standard used to normalize the values reported in Table 1.

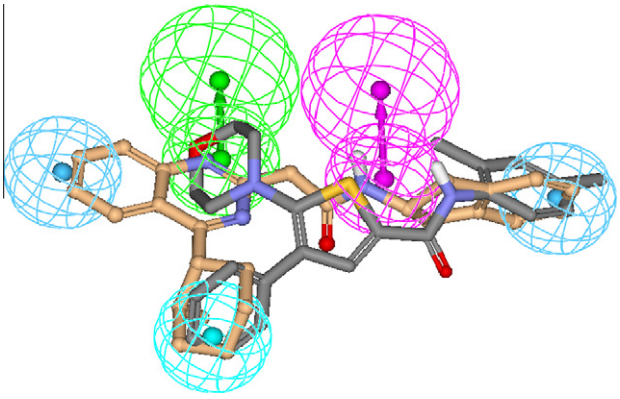

**Figure 5.** Alignment of compound **15** (stick, colored by atom type) to the pharmacophore model. For comparison, one of the derivative utilized to build the model (compound **11**, ball and stick, orange) is also shown.

Following oral administration formulated in 1% methylcellulose and dosed at 3 mg/kg to the male rat, compound **15** showed very low systemic exposure (AUC0-t ~ca. 2 ng h/mL). The hepatic clearance was high (in agreement with the rat in vitro Cli) and approaching the rat liver blood flow (77 mL/min/kg). As a result of the high hepatic Cl and low systemic exposure, the estimated bioavailability was very low (<1%). All brain samples were below the quantitation limit; therefore brain penetration could not be determined. These data show that the PK profile of this novel hit was sub-optimal. This was potentially due to metabolic liability points present in the scaffold which need to be appropriately protected.

In summary, a first series of potent and selective α7 positive allosteric modulators were identified by screening in house diversity. These structures allowed the construction of a novel pharmacophore model for α7 PAMs and to use the derived knowledge to define novel positive modulator templates with the use of lead hopping techniques.

## Acknowledgments

The authors would like to thank colleagues in SMTech and Analytical Chemistry for the support provided and Dr. Gianpaolo Bravi and Dr. Giovanna Tedesco (Computational Chemistry Europe group) for helpful discussion.

## Supplementary data

Supplementary data associated with this article can be found, in the online version, at doi:10.1016/j.bmcl.2010.06.014.

## References and notes

1. Bertrand, D.; Galzi, J. L.; Devillers-Thiery, A.; Bertrand, S.; Changeux, J. P. *Proc. Natl. Acad. Sci. U.S.A.* **1993**, *90*, 6971.
2. Seguela, P.; Wadiche, J.; Dineley-Miller, K.; Dani, J. A.; Patrick, J. W. *J. Neurosci.* **1993**, *13*, 596.
3. Alkondon, M.; Pereira, E. F.; Cortes, W. S.; Maelicke, A.; Albuquerque, E. X. *Eur. J. Neurosci.* **1997**, *9*, 2734.
4. (a) Zarei, M. M.; Radcliffe, K. A.; Chen, D.; Patrick, J. W.; Dani, J. A. *Neuroscience* **1999**, *88*, 755; (b) Frazier, C. J.; Buhler, A. V.; Weiner, J. L.; Dunwiddie, T. V. *J. Neurosci.* **1998**, *18*, 8228; (c) Minana, M. D.; Montoliu, C.; Llansola, M.; Grisolia, S.; Felipo, V. *Neuropharmacology* **1998**, *37*, 847; (d) Albuquerque, E. X.; Pereira, E. F. R.; Braga, M. F. M.; Matsubayashi, H.; Alkondon, M. *Toxicol. Lett.* **1998**, *102–103*, 211; (e) Neubauer, B. A.; Fiedler, B.; Himmelein, B.; Kampfer, F.; Lassker, U.; Schwabe, G.; Spanier, I.; Tams, D.; Bretscher, C.; Moldenhauer, K.; Kurlemann, G.; Weise, S.; tedroff, K.; Eeg, O.; Wadelius, C.; Stephani, U. *Neurology* **1998**, *51*, 1608; (f) Stevens, K. E.; Kem, W. R.; Mahnir, V. M.; Freedman, R. *Psycopharmacology* **1998**, *136*, 320; (g) Adler, L. E.; Olincy, A.; Waldo, M.; Harris, J. G.; Griffith, J.; Stevens, K.; Flach, K.; Nagamoto, H.; Bickford, P.; Leonard, S.; Freedman, R. *Schizophrenia Bull.* **1998**, *24*, 189.
5. Martin, L. F.; Kem, W. R.; Freedman, R. *Psycopharmacology* **2004**, *174*, 54.

6. Briggs, C. A.; McKenna, D. G. *Neuropharmacology* **1998**, *37*, 1095.
7. Lightfoot, A. P.; Kew, J. N. C.; Skidmore, J. *Prog. Med. Chem.* **2008**, *46*, 131.
8. Pavlov, V. A.; Tracey, K. J. *Biochem. Soc. Trans.* **2006**, *34*, 1037.
9. Breining, S. R.; Mazurov, A. A.; Miller, C. *Ann. Rep. Med. Chem.* **2005**, *40*, 3.
10. Leonik, F. M.; Papke, R. L.; Horenstein, N. A. *Bioorg. Med. Chem. Lett.* **2007**, *17*, 1520.
11. Carbonnelle, E.; Sparatore, F.; Canu-Boido, C.; Salvagno, C.; Baldani-Guerra, B.; Terstappen, G.; Zwart, R.; Vijverberg, H.; Clementi, F.; Gotti, C. *Eur. J. Pharmacol.* **2003**, *471*, 85.
12. Virginio, C.; Giacometti, A.; Aldegheri, A.; Rimland, J. M.; Terstappen, G. C. *Eur. J. Pharmacol.* **2002**, *445*, 153.
13. Catalyst 4.10, Accelrys Inc. http://accelrys.com.
14. A Catalyst database (max 50 conformations, FAST) was generated for 1600 randomly selected GSK collection compounds, seeded with 18 α7 positive modulators derivatives structurally related to the compounds shown in Figure 2. The GSK compounds selected at random were assumed to be inactive as positive modulators of the α7 nAChR. Subsequently, this database was screened in silico with the pharmacophore model shown in Figure 4 by utilizing different search conditions (rigid vs flexible mapping), minimum fit to the pharmacophoric features and pharmacophore feature weights (default vs customized values). Hitlists were evaluated in light of the fraction of database compounds retrieved, the number of known actives fished out as well as the overall number of different chemotypes obtained. Results are reported in the Supplementary data.
15. ROCS 2.0, OpenEye Scientific Software Inc. http://www.eyesopen.com/products/applications/rocs.html.
16. multi_smarts_filter, Daylight 4.71 Daylight Inc.
17. Pozzan, A.; Feriani, A.; Tedesco, G.; Capelli, A. M. In *Rational Approaches to Drug Design*; Hoeltje, H.-D., Sippl, W., Eds.; Prous Science, 2001; pp 224–228.
18. Hamming, R. W. *Bell Syst. Tech. J.* **1950**, *26*, 147.
19. Ward, J. H. *J. Am. Stat. Assoc.* **1963**, *58*, 236.
20. All the works involving animals were carried out in accordance with the Animals (Scientific Procedures) Act (1986), European directive 86/609/EEC governing animal welfare and protection and according to internal review performed by the GlaxoSmithKline Committee on Animal Research & Ethics (CARE) and to the company Policy on the Care and Use of Laboratory Animals.